Journal of Solid State Chemistry **162,** 341–346 (2001)
doi:10.1006/jssc.2001.9369, available online at http://www.idealibrary.com on IDEAL®

Low Members of the Intergrowth Tungsten Bronze Family by Partial Substitution of Molybdenum for Tungsten

Lars Kihlborg,[1] Helen Blomqvist, and Margareta Sundberg

Inorganic Chemistry, Stockholm University, SE-106 91 Stockholm, Sweden

DEDICATED TO PROFESSOR PAUL HAGENMULLER ON THE OCCASION OF HIS 80TH BIRTHDAY

Potassium and cesium intergrowth tungsten bronzes $A_xMo_yW_{1-y}O_3$ with $x \lesssim 0.25$ and $y \lesssim 0.65$ have been prepared. By substitution of molybdenum for tungsten the synthesis temperature can be decreased to 600°C and new phases of the structure family prepared. The ITB members designated (1, 3) and (1, 1, 3) have been prepared in relatively phase-pure form, while individual crystals of (1, 2) and (1, 1, 2) have been identified by electron microscopy. These four phases have not been found previously in the ITB bronze systems. © 2001 Elsevier Science

Key Words: **intergrowth tungsten bronzes; oxide bronzes; substitution; electron microscopy; microanalysis.**

INTRODUCTION

The chemical behavior of the elements molybdenum and tungsten is similar in many respects, yet their structural chemistry exhibits distinct differences, despite their similar ionic size. The structure of their stable hexavalent oxides, for example, is quite different: WO_3 has a somewhat distorted ReO_3-type structure while MoO_3 has a unique layer structure. These differences are probably related to the different tendency to form directional bonds, which is higher for molybdenum, resulting in a much larger spread in the M–O bond lengths within the octahedra of MoO_3 compared to those of WO_3. The MoO_3 structure, in which one oxygen in the MoO_6 octahedron is bonded only to one molybdenum, can more easily accommodate this preference. The stability of an ReO_3-type framework is only marginally lower, however, as shown by the possibility to prepare such a structure in a metastable state at low temperatures (1–3). The trioxides form mixed crystals $W_xMo_{1-x}O_3$ over the entire range $0 < x < 1$ and these have ReO_3-related structures, except for $x < 0.05$ where an MoO_3-like structure forms (4).

With respect to reduced phases, it has long been known that tungsten can substitute for molybdenum in the M_nO_{3n-1} shear structure phases (5). The oxides Mo_5O_{14} and $Mo_{17}O_{47}$, with other types of structures, have no counterparts in the W–O system, but W can replace substantial amounts of Mo in these phases (6). Also the two Mo_4O_{11} phases, monoclinic and orthorhombic, tolerate substitution by tungsten, whereby new homologues are formed (7, 8). On the other hand, the oxide $W_{18}O_{49}$ does not seem to have any extended homogeneity range in the ternary system (9).

With alkali (and other electropositive metals) tungsten forms oxide bronzes, A_xWO_3, of four structural types: perovskite-type (PTB), tetragonal potassium tungsten bronze (TTB), hexagonal tungsten bronze (HTB), and intergrowth tungsten bronze (ITB). These have no counterparts in the A–Mo–O system, where molybdenum bronzes of quite different, complex structures are found. Although studies have been made on heterovalent substitution in the tungsten bronzes, for example the formation of fully oxidized Nb- and Ta-substituted phases (10, 11), no investigations seem to have been made previously of isovalent (group 6) substitution in these phases. We have found that molybdenum can substitute for tungsten in PTB, HTB, and ITB. This paper will focus on one type of tungsten bronze, the so-called *intergrowth tungsten bronzes*, ITB, and it will be shown that they can accommodate considerable amounts of molybdenum, whereby new members of the intergrowth bronze family are formed. Preliminary results of the present investigation have been reported at conferences (12, 13).

INTERGROWTH TUNGSTEN BRONZES

The ITB phases, typically forming with the large alkali elements, K, Rb, and Cs, have structures that can be considered as intergrowth of slabs with a distorted WO_3-type structure and those of hexagonal tungsten bronze, HTB (14). The slabs are infinite in two dimensions but have a finite width. The widths of the two types of slabs define a particular member of the family. Two examples of ITB structures are shown in Fig. 1. Different ordered intergrowth structures can conveniently be designated by a series of numbers enclosed by parentheses, indicating the number

[1] To whom correspondence should be addressed. fax: + 46 8 152187. E-mail: larsk@inorg.su.se.

0022-4596/01 $35.00

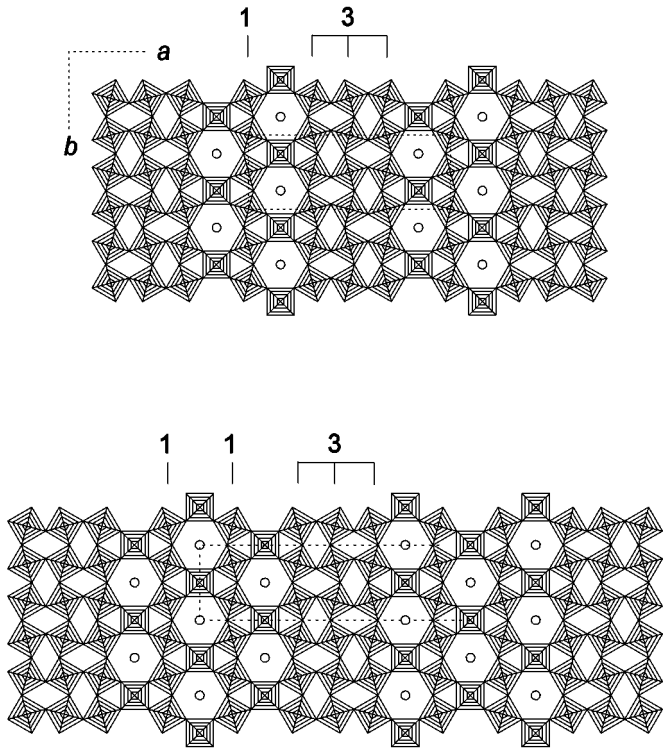

FIG. 1. Models of two ITB structures; (1, 3)-ITB (top) and (1, 1, 3)-ITB (*bottom*), depicted as linked MO_6 octahedra and viewed along the short (3.9 Å) c' axis. The positions of the alkali atoms in the tunnels of the HTB slabs are indicated by circles. The unit cell of the (1, 3) structure is shown, while only half the cell of the *C*-centered (1, 1, 3) structure has been drawn.

of rows of octahedra between (the centers of) the HTB-slab tunnels within a repeating sequence, as exemplified in Fig. 1. Thus, (1, *n*) indicates ITB phases where the HTB elements are two tunnel rows wide, while in the (1, 1, *n*) members they comprise three tunnel rows. Structures with only a single row of hexagonal tunnels in the HTB elements are accordingly designated (*n*). The alkali atoms are located in the hexagonal tunnels of the HTB slabs and the alkali content, *x*, depends on the number of available tunnel sites as well as on the occupancy of these sites. The maximum alkali contents for some ITB phases are given by the expressions:

$$(n)\text{-ITB:} \qquad x_{\max} = 1/(1 + 2n)$$

$$(1, n)\text{-ITB:} \qquad x_{\max} = 2/(4 + 2n)$$

$$(1, 1, n)\text{-ITB:} \quad x_{\max} = 3/(7 + 2n).$$

It can be noted that in all cases $n = 1$ represents the HTB structure, with $x_{\max} = \frac{1}{3}$.

The unsubstituted alkali ITB phases form only at rather high temperatures, 800°C or above (15). In this case ordered phases (1, *n*) with $4 \leq n \leq 14$ have been observed (16), as well as some single-tunnel ones, (*n*), with $7 \leq n \leq 11$ (17). In addition, crystals with more or less ordered superstructures, such as the one represented by (7, 8), as well as completely disordered sequences, have been revealed by high-resolution electron microscopy (HREM), which is a very suitable tool for the study of these phases. The tunnel occupancy by alkali seems to be around 60% in most cases (16, 18, 19).

By substitution of niobium for tungsten according to the formula $A_xNb_xW_{1-x}O_3$ fully oxidized ITB phases—*bronzoids*—can be prepared, but only if the synthesis temperature is increased to 1200°C (20). In these samples ITB-type phases (1, *n*) with $n = 2$–9, (1, 1, *n*) and (1, 1, 1, *n*) phases with $n = 3$–7 have been observed (11). Even the phase (1, 1, 1, 1, 4), an ordered structure where the HTB slabs are five tunnel rows wide, has been seen. Complex superstructures and disorder are quite frequent in many of these crystals.

The samples obtained in the syntheses have mostly been mixtures of crystals of different ITB members; only in a few cases have samples been obtained, which have been reasonably phase-pure, allowing interpretation of the complex X-ray powder pattern.

EXPERIMENTAL

Samples of various composition $A_xMo_yW_{1-y}O_3$ with $A =$ K or Cs were prepared by reaction in sealed silica tubes at 600–900°C, in general for a week. Starting materials were WO_3, MoO_3, K_2MoO_4, and Cs_2WO_4. WO_2, or MoO_2, or in some cases Mo or W, was used as reducing agent. All chemicals were of high purity. The composition of WO_2 was checked by oxidation in a TGA apparatus and the slight oxygen excess found was taken into account. Appropriate amounts of the chemicals were mixed by careful grinding in an agate mortar. The weighed compositions were within the ranges $0.05 \leq x \leq 0.55$, $0.08 \leq y \leq 0.40$ for the potassium system and $0.05 \leq x \leq 0.25$, $0.05 \leq y \leq 0.70$ for the cesium one.

The samples were investigated by X-ray powder diffraction in Guinier–Hägg-type focussing cameras using Cu$K\alpha_1$ radiation and Si as internal standard ($a = 5.430879$ Å). Selected films were read using an automatic film-scanner (21) and evaluated with use of the computer programs SCANPI and PIRUM (22).

Electron microscopy was used extensively for the analysis and characterization of the samples. A JEOL 2000FX-II microscope (operated at 200 kV) with an attached LINK AN10000 EDS system was used for electron diffraction and analysis of individual crystals. HREM studies were made on JEOL JEM-200CX (200 kV) and JEM-3010 (300 kV) microscopes. TEM specimens were prepared by crushing a small part of the sample in a mortar, suspending the powder in *n*-butanol, and putting a drop of the suspension on a holey

carbon film supported by a copper grid and letting the liquid evaporate. Some samples were also studied with a scanning electron microscope (SEM), JEOL JSM-820, with a LINK EDS detector. Electron diffraction (ED) patterns were simulated with upgraded versions of the program DIFPAT (23), while for the simulation of HREM images a locally modified version of the program suite SHRLI (24) was used.

In the EDS analysis the peaks K*K*, Mo*K* or Mo*L*, Cs*L* and W*L* were used for quantification. In the system Cs–Mo–W–O, crystals of $Cs_2Mo_3O_{10}$ and $Cs_6W_{11}O_{36}$ were used as standards and the corrections to the Cs/Mo and Cs/W ratios were applied to the analyses. The EDS analyses in the TEM and SEM microscopes were in general in good agreement with the gross compositions of the samples.

RESULTS

Our experiments indicated that substitution of molybdenum for tungsten can take place and that the temperature range for the formation of ITB phases thereby is lowered considerably. Mo-containing ITB crystals were obtained in the whole range investigated, 600–900°C. The various ordered ITB phases found in samples heated at different temperatures are listed in Table 1. The ordered phases identified in the K–Mo–W–O system were only of the type (1,*n*), but in the Cs system also crystals of (1, 1, *n*)-ITB, i.e., triple-tunnel structures, were observed. This difference may be accidental, however, as disordered fragments containing triple-tunnels have been seen in HREM images in the potassium system. It is obvious from Table 1 that phases with lower *n* values are formed at the lower temperatures.

TABLE 1
ITB Phases Observed in the Systems (a) $K_xMo_yW_{1-y}O_3$ and (b) $Cs_xMo_yW_{1-y}O_3$

ITB member	x_{max}	EDS analyses straddle		Formation temperature/°C
		x	*y*	
		(a) $K_xMo_yW_{1-y}O_3$		
(1, 7)	0.111	0.08	0.10	900
(1, 6)	0.125	0.08–0.09	0.07–0.23	800–900
(1, 5)	0.143	0.08–0.10	0.08–0.16	700–900
(1, 4)	0.167	0.10–0.13	0.08–0.30	700–800
(1, 3)	0.200	0.09–0.16	0.08–0.32	600–750
		(b) $Cs_xMo_yW_{1-y}O_3$		
(1, 6)	0.125	0.06–0.09	0.09–0.16	725
(1, 5)	0.143	0.07–0.10	0.02–0.15	700–800
(1, 4)	0.167	0.08–0.15	0.14–0.47	650–800
(1, 3)	0.200	0.11–0.22	0.18–0.60	600–750
(1, 2)	0.250	0.20–0.24	0.37–0.60	600–650
(1, 1, 3)	0.231	0.14–0.23	0.30–0.64	600–650
(1, 1, 2)	0.273	0.25	0.67	600

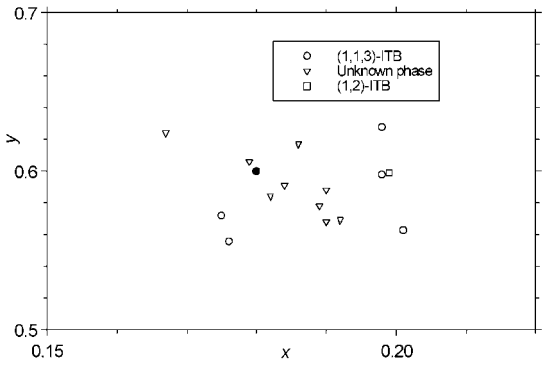

FIG. 2. Plot of EDS analyses of 15 crystals from a sample in the Cs system with $x = 0.18$, $y = 0.60$ (black dot). Each point represents the mean of two or three measurements on the same crystal. The triangles ("unknown phase") indicate crystals that were not positively identified, because they were laying in an unfavorable orientation. The X-ray powder pattern of this sample shows mainly the lines of (1, 1, 3)-ITB.

The syntheses in the potassium and cesium systems covered somewhat different compositional ranges, as stated above. In the Cs system more consideration was given to high values of *x* and *y* and low temperatures (600 and 650°C). This may be the main reason for the differences seen between Tables 1a and 1b. We do not have any reason to believe that the two systems behave differently with respect to the ITB members formed.

A typical plot of EDS analyses of different crystals in one sample is shown in Fig. 2.

Although ITB crystals usually form as flat needles with the needle axis being **c** and **a** going perpendicular to the flat surface, they have no marked cleavage and fragments of different orientations can usually be found in the TEM specimens. The ED patterns of the various ITB structures can conveniently be distinguished in the favorable [001] orientation by measuring the ratio b^*/a'^*, where a'^* is the distance between the *h*00 spots, and can be confirmed by observing the presence or not of *C*-centering, i.e., $r_c = 2$ or 1, respectively (17). Values for a few relevant *n*-values are given in Table 2. It should be noted that the observed ratios b^*/a'^* are fairly close to the ideal ones. ED patterns of some

TABLE 2
$(b^*/a'^*)_{ideal}$ and r_c for Selected ITB Members[a]

n	(*n*)	(1, *n*)	(1, 1, *n*)
2	1.37 1	2.23 2	3.10 1
3	1.87 2	2.73 1	3.60 2
4	2.37 1	3.23 2	4.10 1
5	2.87 2	3.73 1	4.60 2
6	3.37 1	4.23 2	5.10 1

[a] $r_c = 1$, primitive cell; $r_c = 2$, *C*-centered unit cell; $a = r_c a'$.

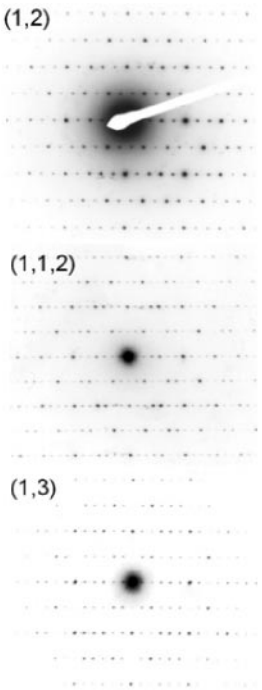

FIG. 3. Electron diffraction patterns of three Cs-ITB members. [001] zones; a^* horizontally and b^* vertically.

low-member phases recorded in the [001] orientation are shown in Fig. 3.

Crystals with a high Mo content, however, have a pronounced cleavage perpendicular to a and it is difficult to find fragments in the crushed samples that can be oriented perpendicular to **a**. They are mostly found as thin plates oriented close to the [100] zone. The [100] zone is practically identical for the different ITB members, but it is possible to distinguish between them by tilting away from this zone to other recognizable zones and measuring the tilting angle. Simulated ED patterns are very helpful for the zone identification.

In the samples with high x values ($x \geq 0.2$) crystals of pure HTB-type were often encountered. These could also contain substantial amounts of Mo substituting for W.

In addition to the distinct ED patterns observed, patterns with more or less pronounced streaking along a^* were frequently seen, indicating disorder in the intergrowth sequence, as reported previously for the unsubstituted ITBs (14, 17) as well as for the Nb-substituted bronzoids (11). Such disorder can also be seen in the HREM images displayed in Figs. 4 and 5.

The X-ray powder patterns of the ITB phases are quite complex due to the long a axis. Powder patterns of mixtures of several ITB members are therefore difficult to interpret. Many of the samples prepared in this investigation contained one dominating phase, however, and the lines from this could then be identified and indexed. Some unit cell dimensions obtained in this way for a few members are given in Table 3. It should be pointed out that the size of the unit cell depends on x and y as well as on the size of the alkali atoms. Only in the case in which a single phase has been obtained, with no additional lines from extraneous phases, can the composition be inferred from the preparation, however, and this is rarely the case in these systems. The values obtained by EDS are measured on a rather limited number of crystals and do not give a statistically significant value for the composition of the whole sample. Any discussion of the variation of the unit cell vs composition must therefore be done with caution. It seems clear from Table 3, however, that the substitution of Mo for

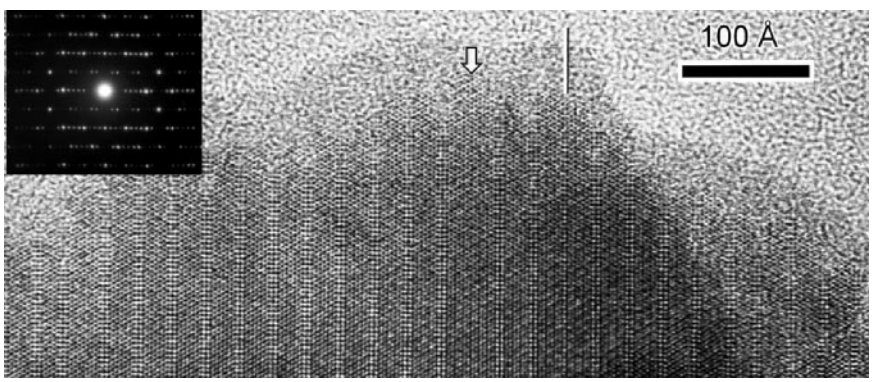

FIG. 4. An HREM image (with the ED pattern inserted) of a crystal fragment, essentially (1,1,3)-ITB, from a sample $Cs_{0.22}Mo_{0.65}W_{0.35}O_3$ prepared at 650°C. The image is taken along the c axis close to Scherzer focus and the supporting carbon film is overlapping. The WO_3 slabs are best seen in the thicker part as vertical rows of pairs of white dots (i.e., the spacing between the three rows of metal atoms), while the HTB elements give a hexagonal pattern of black dots, because the electron scattering of the Mo/W and Cs atoms is similar. The white arrow indicates a defect where the HTB slab is six tunnel rows wide instead of the normal three. The white line points to another defect: a WO_3-type slab that is only two octahedra wide. There are further deviations from periodicity to the very left.

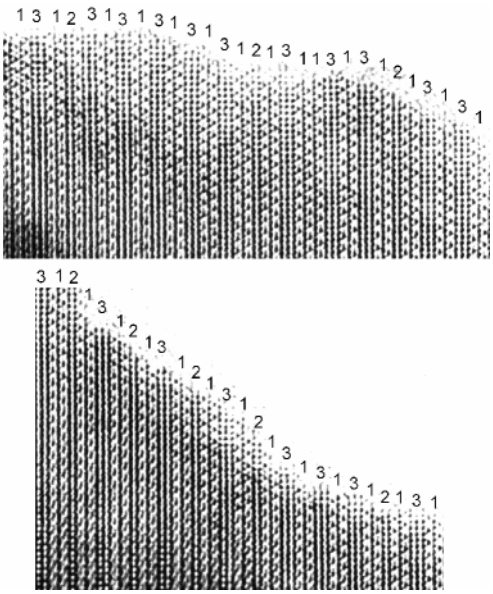

FIG. 5. Two connecting parts of an HREM image of a crystal from a sample of gross composition $K_{0.20}Mo_{0.40}W_{0.60}O_3$ prepared at 700°C. Atoms appear as black dots. The n values indicated show considerable disorder. While the sequence (1, 3) predominates, there is, for example, a part with the superstructure (1, 2, 1, 3).

W decreases the a axis and increases the c axis for the (1, 4) phase. The b axis also decreases somewhat in the Cs case. The a and c axes are longer in the Cs phases than in the corresponding K phases, which is in agreement with the observations on unsubstituted HTB (25).

DISCUSSION

We have shown that the tungsten atoms in the ITB phases can be replaced by molybdenum up to (at least) 65%.

TABLE 3
Unit Cell Dimensions for Selected ITB Phases As Determined by X-Ray Powder Diffraction[a]

	Synthesis data					
Phase	x	y	Temp./°C	a/Å	b/Å	c'/Å
Cs-(1, 1, 3)	0.18	0.60	600	52.710	7.282	3.980
K-(1, 3)	0.08	0.20	650	19.948	7.293	3.898
Cs-(1, 3)	0.20	0.60	600	20.046	7.293	3.959
K-(1, 4)	0.10	0.20	700	47.261	7.297	3.902
Cs-(1, 4)	0.18	0.50	685	47.466	7.315	3.938
K-(1, 4)[b]	0.10	0	800	47.34	7.30	3.867
Cs-(1, 4)[c]	0.09	0	840	47.539	7.344	3.918

[a] The values given for a, b, and c' are accurate to the last figure. Weak spots in the ED patterns indicate that the c axis is doubled ($c = 2c'$) but this doubling does not show up in the X-ray powder patterns (14).

[b] Ref. (14).

[c] Ref. (16).

This extends their temperature range of formation downward by at least 200°C (experiments below 600°C were not carried out in this study). In the samples heated at low temperatures new ITB members form, in which the WO_3-type slabs are narrower and the proportion of the HTB structure is higher. This tendency has been observed previously for the pure tungsten ITBs (16). In that case, samples with the same initial composition ($x = 0.06$) were heated at different temperatures. The ITBs formed at 925–950°C had average n values in the range 7.5–8, while those heated at 840–900°C had $n = 4$–5.

The ITB members (1, 3), (1, 2), (1, 1, 3), and (1, 1, 2) have not been observed in the unsubstituted bronzes. In the niobium-substituted bronzoids, $A_xNb_xW_{1-x}O_3$, these members do appear, however, although the temperature in this system has to be increased to 1200°C (11), as mentioned above. The ITB formation range is restricted to $x \approx 0.1$. It is obvious that the vapor pressure of the additional oxide is of great importance for the formation temperature. The niobium oxides are not easily vaporized and require an increased temperature. MoO_3, on the other hand, has a much higher vapor pressure than WO_3, and the temperature can be lowered.

The degree of filling of the HTB tunnels by alkali, which can be deduced from the structure and the EDS analysis, are in the present experiments between 50–100%. The majority of the crystals have an occupancy around 60–70%, which is in line with previous studies on unsubstituted ITBs, as mentioned above. Only in a few crystals has the measured alkali content approached 100% occupancy.

The sample can adapt to the gross composition either by varying the proportion of HTB elements, and thereby tunnels, in the structure or by varying the occupancy in the tunnels. As the occupancy in most cases stays within a certain range it seems that this is a favorable degree of filling to stabilize the HTB elements. The Mo content seems to have little influence on this. However, the formation mechanism of the ITB phases is not well known and is probably quite complex, depending on the vapor pressures of the components and the amounts available at each stage of the crystal growth. Once a certain ITB member has formed, its transformation into another, more stable phase is likely to be a sluggish process, particularly at the low temperatures used in the present study.

It would be of great interest to know if there is a segregation of molybdenum and tungsten in the ITB crystals or if the distribution is completely statistical. This requires well-ordered crystals of good quality, large enough for single-crystal X-ray diffraction. Relatively large crystals have been obtained in the potassium system, but according to preliminary diffraction studies of these their quality has not been high enough for single-crystal work. It is possible that Rietveld analysis of suitable X-ray powder patterns of one of the lowest members can give an answer and efforts in this direction will be made.

ACKNOWLEDGMENTS

The participation of Dr. L.-J. Norrby and Mr. O. Ringaby in early stages of this investigation is greatly acknowledged. Thanks are also directed to Dr. M. Nygren for carrying out analyses of commercial WO_2 by thermal gravimetry, to Dr. K. Jansson for assistance with the EDS systems, and to Mrs. J. Östlund for photographic work. This investigation forms a part of a research project financially supported by the Natural Science Research Council (NFR).

REFERENCES

1. E. M. McCarron, III, *Chem. Commun.* **4,** 336 (1986).
2. G. Svensson and L. Kihlborg, *React. of Solids* **3,** 33 (1987).
3. F. Harb, B. Gérand, G. Nowogrocki, and M. Figlarz, *Solid State Ionics* **32/33,** 84 (1989).
4. E. Salje, R. Gehlig, and K. Viswanathan, *J. Solid State Chem.* **25,** 239 (1978).
5. A. Magnéli, B. Blomberg-Hansson, L. Kihlborg and G. Sundkvist, *Acta Chem. Scand.* **9,** 1382 (1955).
6. T. Ekström, *Mater. Res. Bull.* **7,** 19 (1972).
7. F. Portemer, M. Sundberg, L. Kihlborg, and M. Figlarz, *J. Solid State Chem.* **103,** 403 (1993).
8. L. Kihlborg, B.-O. Marinder, M. Sundberg, F. Portemer, and O. Ringaby, *J. Solid State Chem.* **111,** 111 (1994).
9. T. Ekström, E. Salje, and R. J. D. Tilley, *J. Solid State Chem.* **40,** 75 (1981).
10. A. Deschanvres, M. Frey, B. Raveau, and J.-C. Thomazeau, *Bull. Soc. Chim. Fr.* 3519 (1968).
11. R. Sharma, *Chem. Commun. Univ. Stockholm* No. 3, 1–42 (1985).
12. L. Kihlborg, L.-J. Norrby, and M. Sundberg, Electron Microscopy 96, Proceed. EUREM-11, Dublin, Ireland, 26–30 August, 1996, II–119.
13. H. Blomqvist and M. Sundberg, Proceed. SCANDEM-98, Esboo & Helsinki, Finland, 7–10 June, 1998, p. 145.
14. A. Hussain and L. Kihlborg, *Acta Crystallogr. A* **32,** 551 (1976).
15. A. Hussain, *Chem. Commun. Univ. Stockholm* No. 2, 1–44 (1978).
16. L. Kihlborg, M. Fernandez, Y. Laligant and M. Sundberg, *Chem. Scr.* **28,** 71 (1988).
17. L. Kihlborg, *Chem. Scr.* **14,** 187 (1978–79).
18. A. Hussain, *Chem. Scr.* **11,** 224 (1977).
19. A. Hussain, L. Permér, and L. Kihlborg, *Eur. J. Solid State Inorg. Chem.* **31,** 879 (1994).
20. R. Sharma and L. Kihlborg, *Mater. Res. Bull.* **16,** 377 (1981).
21. K. E. Johansson, T. Palm, and P.-E. Werner, *J. Phys. E, Sci. Instrum.* **13,** 1289 (1980).
22. P.-E. Werner, *Arkiv Kemi* **31,** 513 (1969).
23. A. J. Skarnulis, G. Liljestrand, and L. Kihlborg, *Chem. Commun. Univ. Stockholm* No. 1, 1–27 (1979).
24. M. A. O'Keefe, P. R. Buseck, and S. Iijima, *Nature* (*London*) **274,** 322 (1978).
25. L. Kihlborg and A. Hussain, *Mater. Res. Bull.* **14,** 667 (1979).